SUPER-RESOLUTION RADAR TOMOGRAPHIC IMAGING WITH EXPLOITING SPATIAL DIVERSITY

Hongbo Sun[1], Hongchuan Feng[2], Yilong Lu[2]

[1]Institute for Infocomm Research, Agency for Science, Technology and Research, Singapore
[2]School of Electrical and Electronic Engineering, Nanyang Technological University, Singapore

ABSTRACT

It is well known that the resolution of conventional radar is typically limited by the bandwidth of adopted waveform. However, we should not forget that the potential spatial resolution that radar can achieve could be much better, more precisely, in the order of sub-wavelength. Such radar operating ^{0}mode is called radar tomography, which exploits the spatial diversity, instead of large waveform bandwidth, to achieve super high spatial resolution. Although the theory of radar tomography had been developed for decades, very few experimental validations were reported in public literatures. In this paper, the investigations on radar tomographic imaging are conducted and validated with the measurements in microwave anechoic chamber. The spatial resolutions achieved in the experiments show good agreement with theoretical results.

Index Terms — *Radar tomography, microwave imaging, synthetic aperture radar*

1. INTRODUCTION OF RADAR TOMOGRAPHY

Synthetic aperture radar (SAR) imaging has been widely used in both military and civilian applications [1][2]. It is well known that in typical SAR imaging, the range resolution is determined by the signal bandwidth, and the cross-range resolution is determined by the angular integration which is normally chosen to be equal to the range resolution. However, the potential spatial resolution that radar can achieve could be much better. A special mode of imaging technique, tomographic imaging, has been developed for medical applications since 1970s, which was also known as computer aided tomography [3] or computerized tomography [4]. In 1980s, the principle of tomographic imaging was introduced into radar applications [5][6]. Different from the SAR imaging whose spatial resolution is roughly limited by the signal bandwidth, tomographic imaging is quite unique as it can provide super high spatial resolution (up to one quarter wavelength) with only exploiting spatial diversity. It is attractive because potentially very high-resolution image can be formed by a radar with narrowband waveforms (as low as a single-tone signal), which means very simple hardware structures and low cost.

There are two image reconstruction approaches for radar tomography: direct Fourier approach and matched filter approach. Direct Fourier approach is based on the projection slice theorem [5][7]. As illustrated in Fig. 1, assuming $f(x,y)$ is the 2-D scattering coefficient to be imaged, the Fourier transform of a parallel projection of $f(x,y)$ along angle θ gives a slice of its two-dimensional Fourier transform $F(u,v)$, along the same angle θ w.r.t. the *u*-axis. In other words, the Fourier transform of $P_\theta(t)$ gives the values of $F(u,v)$ along the line B in Fig. 1.

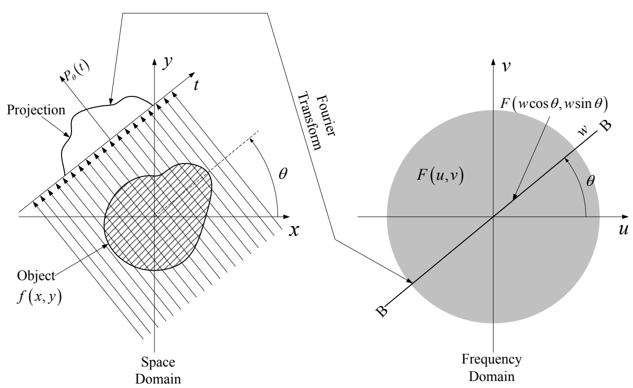

Fig. 1. Illustration of Fourier slice theorem

Matched filter approach [8], which was also called beamforming algorithm [9], is an intuitive signal processing technique in the brute force way. For the image reconstruction in spatial domain, matched filter approach simply attempts to compensate the signal's expected phase delay for each grid of the scene. For a grid containing the target, all echoes from this grid can be adapted to a constant phase with proper phase weights. Summing up all these phase weighted echoes will produce an image of the target.

Thanks for the efficiencies of fast Fourier transform (FFT), the direct Fourier technique is much superior to the matched filter technique in terms of the computational load. However, the application of direct Fourier technique has many constraints. First, the direct Fourier reconstruction is derived based on plane wave assumption. The distance between the target (or the image scene) and the radar should satisfy far-field conditions. Second, before applying 2-D inverse FFT for image reconstruction, the polar samples in spatial frequency domain must be interpolated into Cartesian grids. The interpolation error may affect the final image quality. In addition, the direct Fourier reconstruction uses the transformation between spatial domain and spatial frequency domain. The image scene is limited within a certain unambiguous area. Outside this area the spatial ambiguity will occur. Relatively the matched filter technique is much more flexible and won't suffer from these constrains. Thus, the matched filter technique is used in this paper.

Although the principle of radar tomographic imaging has been developed many years ago, there were not many experimental results in public literatures [7][8][10]. Based on the preliminary analyses conducted by the authors in [11], in this paper, more extensive investigations on radar tomographic imaging are conducted and validated with the measurements in microwave anechoic chamber.

2. POINT SPREAD FUNCTION ANALYSIS

First we look at the point spread function (PSF) of radar tomography processing when a single-tone continuous wave (CW) signal is used with 360° observation. In 2-D spatial frequency domain, the measurement samples of single-tone frequency are at a circle around the origin with a radius of $\lambda/2$, where λ is the signal wavelength. The corresponding PSF is the 2-D inverse Fourier transform of the data on this circle, which can be derived in polar coordinates as [4].

$$h(r)=\frac{2}{\lambda}\int_0^{2\pi}\exp\left(-j\frac{4\pi r}{\lambda}\cos\theta\right)d\theta=\frac{4\pi}{\lambda}J_0\left(\frac{4\pi r}{\lambda}\right) \quad (1)$$

where $J_0(x)$ is the zero-order Bessel function. The first null of $J_0(x)$ is at $x_0=2.4048$. So the null-to-null width of PSF mainlobe, i.e., the spatial resolution of tomographic imaging with single-tone signal, is

$$\rho=2r_0=\frac{4.8096\lambda}{4\pi}=0.3827\lambda\approx\frac{2}{5}\lambda \quad (2)$$

Fig. 2 illustrates the PSF of tomographic imaging when 1GHz single-tone frequency is used. The 3dB resolution is about $\lambda/4$, and the first sidelobe is at about -8dB.

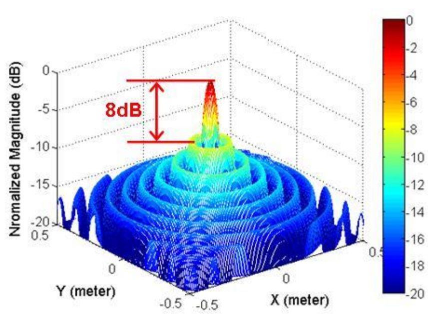

Fig. 2. PSF for one single-tone frequency and 360° observation

This simulation result shows that very high spatial resolution can be achieved by tomographic imaging with only one single-tone frequency. However, the high sidelobe level is still an issue to be solved. It was observed that including more frequency components can significantly change the distribution of sidelobes. When more than one single-tone frequencies are adopted, the PSF of tomographic imaging is

$$h(r)=\sum_{i=1}^{M}\frac{4\pi}{\lambda_i}J_0\left(\frac{4\pi r}{\lambda_i}\right) \quad (3)$$

where M is number of frequencies. There is no analytical expression for (3). Some example PSFs for two single-tone frequencies with different frequency spacing were presented in [11]. Interestingly, with a number of single-tone frequencies with fixed frequency spacing, the high sidelobes of PSF in tomographic imaging can be effectively suppressed. As an example, Fig. 3 depicts the PSF when five frequencies, 3GHz, 3.5GHz, 4GHz, 4.5 GHz and 5GHz, are used, and Fig. 4 shows the corresponding range cut of PSF. It can be seen that the sidelobes near the mainlobe are much lower than those in single frequency PSF. However, high ambiguous lobes appear due to the frequency discontinuity. The positions of ambiguous range are at

$$R_a=\frac{c}{2\Delta f}\cdot i,\quad i=1,2,3,\cdots \quad (4)$$

where Δf is frequency increment. In Fig. 3 and Fig. 4, $\Delta f=0.5\text{GHz}$, so the first ambiguity is 0.3m away from the mainlobe. To avoid the range ambiguity, Δf should be smaller than $c/2R_a$, where R_a is the maximum radius of target or area to be imaged.

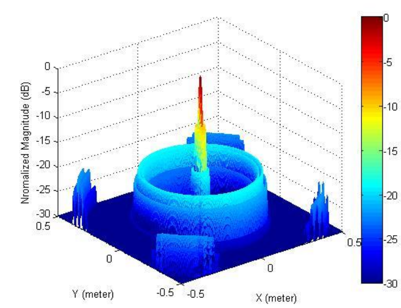

Fig. 3. PSF for 5 frequencies and 360° observation

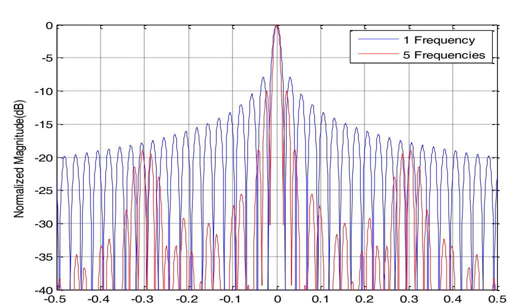

Fig. 4. Range cut of PSF for 5 frequencies and 360° observation

3. ANGULAR SAMPLING INTERVAL

Radar tomographic imaging exploits spatial diversity to achieve the high spatial resolution. Its angular sampling interval should satisfy the sampling theorem, i.e., the phase difference between two adjacent samples should be less than π to fully recover a complex signal from discrete samples. Fig. 5 shows the angular sampling scenario for a scatterer moves from *A* to *A'*, where the phase experiences the steepest variation. Assuming the maximum radius of the image scene is r_m, the angular increment between two adjacent samples is $\Delta\theta$, it can be easily derived that the maximum angular sampling interval should satisfy

$$\Delta\theta < \lambda/4r_m \tag{5}$$

From Eq.(5) we can know that finer angular sampling interval is required if the image scene is larger.

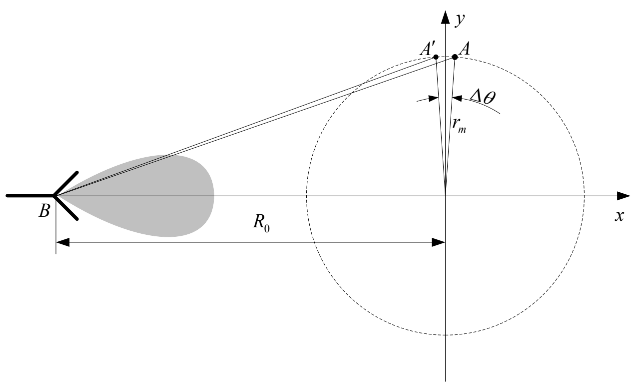

Fig. 5. The steepest phase variation scenario in angular sampling

Numerical simulations are conducted to validate the effects of angular interval. Assuming a 1GHz single-tone frequency signal is used and a point target is at (0.5m, 0m), Fig. 6(a)(b) show the tomographic imaging results with 5° and 10° angular sampling intervals respectively. It can be seen that the maximum allowable radius of image scene is reduced with larger angular sampling interval.

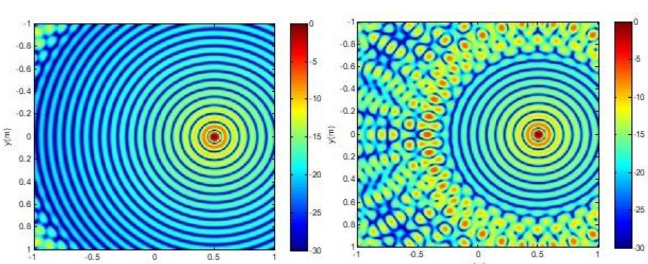

(a) (b)

Fig. 6. PSF of single-tone frequency with (a) 5º and (b) 10° angular sampling interval

4. EXPERIMENTAL VALIDATION

Experimental validations for the radar tomographic imaging are conducted in a microwave anechoic chamber. In our measurements, a microwave network analyzer is used as a radar to transmit/receive the single or multi-frequency CW signals. The targets are fixed on top of a rotator, which is about 3m away from the antennas. The measurement system setup is illustrated in Fig. 7.

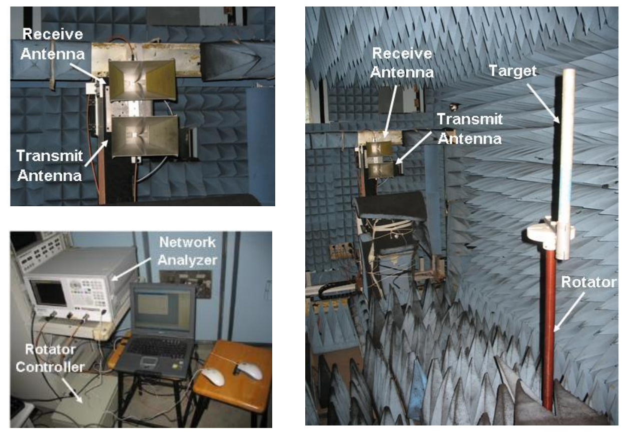

Fig. 7. Setup for tomography imaging experiments

First the measured image of a metal rod is presented in Fig. 8(a) when 2.5GHz single frequency, 360° scan and 1° sampling interval are used. Note that the direct coupling signal from transmit antenna has been cancelled from the received signal before the tomographic imaging. We can see a strong reflection at (0.23m, 0.08m) which is from the metal rod, and a weaker reflection from (0m, 0m) which is from the rotator. To get the image of metal rod only, a separate measurement is conducted for the empty scene without the rod, then the empty scene image is subtracted from the original image and the result is plotted in Fig. 8(b). It can be seen that the image of metal rod is quite close to the theoretical PSF shown in Fig. 2. We also note that with only one single-tone frequency, the sidelobe levels in Fig. 8(a) and (b) are quite high. To reduce the sidelobes, a wideband signal which consists of 201 frequencies from 2.5GHz to 3.5GHz is used. The original image and the image after empty scene are shown in Fig. 8(c) and (d). It can be clearly observed that the sidelobe levels are much lower than those in Fig. 8(a)(b).

Sometimes full 360° scan may be impractical due to some constraints. With less spatial diversity, the spatial resolution will decrease and the sidelobes will increase. To validate this, Fig. 9(a)(b) show the measured PSFs for one 2.5GHz single-tone signal with 120° and 60° scans respectively. From them we can clearly see that the difference in mainlobe spreading and sidelobe distribution. For such cases, frequency diversity can be used to compensate the spatial diversity and reduce the sidelobe level. Fig. 9(c) shows the measured PSF with 60° angular diversity when a wideband waveform (201 frequencies in the band from 2.5GHz to 3.5GHz) is adopted. For comparison, Fig. 9(d) shows the simulated PSF. We can see significant improvement in the sidelobe level when comparing Fig. 9(c)(d) to Fig. 9(b). Thus, in practical applications, it is desired to adopt both spatial and frequency diversities for achieving better performance.

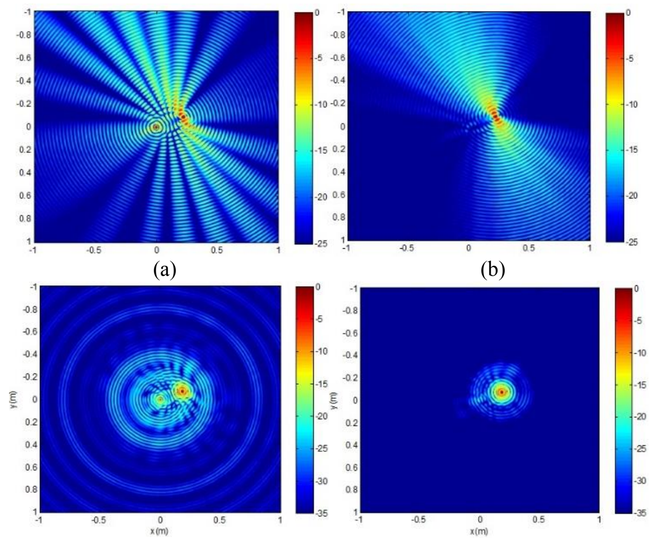

(a) (b) (c) (d)

Fig. 8. Measured images of a metal rod with 360º scan.
(a) Original image of single frequency 2.5GHz;
(b) The image of single frequency after empty scene subtraction;
(c) Original image of multi-frequency 2.5-3.5GHz;
(d) The image of multi-frequency after empty scene subtraction.

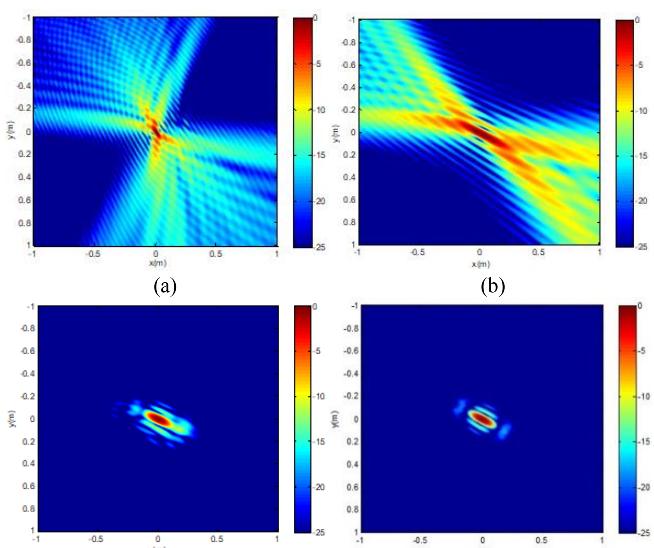

(a) (b) (c) (d)

Fig. 9. Measured PSF with different angular diversity
(a) Single frequency 2.5GHz, 120° integration;
(b) Single frequency 2.5GHz, 60° integration;
(c) Multiple frequencies from 2.5-3.5GHz, 60° integration;
(d) Simulated PSF for (c).

Many more measurements for various targets have been conducted and will be presented in the conference, due to the limitation of paper length.

5. CONCLOSION

The potentials of super high resolution for radar tomographic imaging, which exploits the spatial diversity instead of large signal bandwidth, are investigated in this paper. It is demonstrated that the spatial resolution up to one-quarter wavelength can be achieved even with one single-tone frequency signal, and if larger bandwidth is available, the sidelobe level can be reduced. This is very attractive for radar imaging, particularly the short range surveillance applications.

6. REFERENCE

[1] M. Soumekh, Synthetic Aperture Radar Signal Processing with MATLAB Algorithms, New York: J. Wiley, 1999.

[2] H. Sun; M. Shimada; F. Xu, “Recent advances in synthetic aperture radar remote sensing - systems, data processing, and applications”, IEEE Geoscience and Remote Sensing Letters, vol. 14, no. 11, pp. 2013-2016, November 2017.

[3] H. J. Scudder, “Introduction to computer aided tomography”, Proceedings of the IEEE, vol. 66, no. 6, pp. 628-637, June 1978.

[4] A. C. Kak, M. Slaney, Principles of Computerized Tomographic Imaging, New York: IEEE Press, 1988.

[5] D. L. Mensa, S. Halevy, G. Wade, “Coherent Doppler tomography for microwave imaging”, Proceedings of the IEEE, vol. 71, no. 2, pp. 254-261, February 1983.

[6] D. C. Munson Jr., J. D. O'Brien, W. K. Jenkins, “A tomographic formulation of spotlight-mode synthetic aperture radar”, Proceedings of the IEEE, vol. 71, no. 8, pp. 917-925, August 1983.

[7] D. Mensa, G. Heidbreder, “Bistatic synthetic-aperture radar imaging of rotating objects”, IEEE Transactions on Aerospace and Electronic Systems, vol. 18, no. 4, pp. 423-431, July 1982.

[8] M. C. Wicks, B. Himed, J. L. E. Bracken, H. Bascom, J. Clancy, “Ultra narrow band adaptive tomographic radar”, 2005 IEEE International Workshop on Computational Advances in Multi-Sensor Adaptive Processing, Puerto Vallarta, Mexico, pp. 36-39, December 2005.

[9] D. L. Mesna, High Resolution Radar Cross-Section Imaging, Norwood, MA: Artech House, 1991.

[10] S. L. Coetzee, C. J. Baker, H. D. Griffiths, “Narrow band high resolution radar imaging”, 2006 IEEE Conference on Radar, Verona, NY USA, pp. 622-625, April 2006.

[11] H. Sun; H. Feng; Y. Lu, "High resolution radar tomographic imaging using single-tone CW signals", 2010 IEEE Radar Conference, Arlington, VA, USA, May 2010.